UCRL-JC-128831 Rev. 1
PREPRINT

Evaluation of the Effect of Meteorological Data Resolution on Lagrangian Particle Dispersion Simulations Using the ETEX Experiment

J.S. Nasstrom
J.C. Pace

This paper was prepared for submittal to
Atmospheric Environment

January 1998

Lawrence Livermore National Laboratory

EVALUATION OF THE EFFECT OF METEOROLOGICAL DATA RESOLUTION ON LAGRANGIAN PARTICLE DISPERSION SIMULATIONS USING THE ETEX EXPERIMENT

JOHN S. NASSTROM and JOHN C. PACE
Atmospheric Science Division, Lawrence Livermore National Laboratory
Mail stop L-103, P.O. Box 808, Livermore, CA 94551-0808 USA
Tel: (510) 423-6738, Fax: (510) 423-4908, Email: jnasstrom@llnl.gov

Abstract — This paper presents results from a series of numerical experiments designed to evaluate operational mesoscale dispersion model simulations, and to investigate the effect of different temporal and spatial resolution of meteorological data from numerical weather prediction models on these simulations. Results of Lagrangian particle dispersion simulations of the first tracer release of the European Tracer Experiment (ETEX) are presented and compared to measured tracer concentrations. The use of higher resolution European Center for Medium-Range Weather Forecasts (ECMWF) model analyzed data produced significantly better agreement between the dispersion model predicted concentrations and the ETEX measurements than the use of lower resolution Navy Operational Global Atmospheric Prediction System (NOGAPS) forecast data. Numerical experiments were performed in which the ECMWF model data with lower vertical resolution (4 instead of 7 levels below 500 mb), lower temporal resolution (12 instead of 6 hour intervals), and lower horizontal resolution (2.5 instead of 0.5 deg) were used. Degrading the horizontal or temporal resolution of the ECMWF data resulted in decreased accuracy of the dispersion simulations. These results indicate that flow features resolved by the numerical weather prediction model data at approximately 45 km horizontal grid spacing and 6 hour time intervals, but not resolved at 225 km spacing and 12 hour intervals, made an important contribution to the mesoscale dispersion.

Key words — Lagrangian stochastic dispersion model, numerical weather prediction models, European tracer experiment, mesoscale dispersion.

1. INTRODUCTION

Motivated by the Chernobyl accident, the European Tracer Experiment (ETEX) was conducted to evaluate and improve real-time continental-scale forecasting of meteorological and hazardous-material air concentration fields (Nodop *et al*., 1997). Model evaluations and inter-comparisons were done in two phases: a real-time study and a post-experiment study, called the Atmospheric Transport Model Evaluation Study II, ATMES II (Girardi *et al*., 1997). During the real-time phase a perfluorocarbon tracer gas was released from Monterfil in northwestern France. Participating modeling groups with access to real-time meteorological data then made predictions, in a simulated emergency response mode, of the concentration of a tracer gas at 168 ground-level sampling locations in 17 European countries. In the ATMES II study, modeling groups were asked to make the same predictions using a common source of meteorological data fields from the European Center for Medium-Range Weather Forecasts (ECMWF), without the time restrictions of the real-time phase. Two separate ETEX tracer releases and experiment periods were used for real-time model evaluation study. The first of these periods (23-27 Oct. 1994) was used for the ATMES II study and this work.

The U.S. Department of Energy's Atmospheric Release Advisory Capability (ARAC) program at Lawrence Livermore National Laboratory participated in both the real-time and ATMES II model evaluation studies. ARAC is an operational emergency-response service, providing real-time calculations of the dispersion of hazardous material if there is an accidental release to the atmosphere. These calculations are made with a 3-D Lagrangian dispersion model based on the advection-diffusion equation using meteorological fields obtained from diagnostic or prognostic meteorological models. This modeling system has been shown to be a valuable tool for assessing the airborne hazard from events such as the Chernobyl accident (Gudiksen *et al*., 1989). It has been evaluated in the past versus several accidental atmospheric releases and tracer experiments (Sullivan *et al*., 1993).

ARAC used two different sources of meteorological data fields and different versions of the Lagrangian particle dispersion model during the two ETEX model evaluation studies, and achieved better results in the second study (ATMES II). In the real-time model evaluation study, during Oct. 1994, ARAC used gridded analysis and forecast meteorological data from the Navy Operational Global Atmospheric Prediction System (NOGAPS) at 2.5 degree latitude, longitude horizontal grid spacing, at 12-hr intervals, and at the standard vertical pressure levels (4 levels below 500 mb). In ATMES II, ARAC used higher resolution ECMWF model gridded analysis data at 0.5 degree grid spacing, at 6 hr intervals, and at 14 vertical levels below 500 mb. In the real-time study, ARAC used the ADPIC (Atmospheric Dispersion Particle-In-Cell) dispersion model (Lange, 1989). In ATMES II, ARAC used a newer RDM-ADPIC model (Ermak *et al*., 1995; Nasstrom, 1995) which solves the advection-diffusion equation using a Lagrangian stochastic, random displacement method (RDM). The model-predicted air concentrations compared fairly well to measured values in the real-time study. However, the model results from ATMES II using higher resolution, analyzed ECMWF meteorological data and RDM-ADPIC showed significant improvement from the real-time study.

Previous studies (e.g., Brost *et al.*, 1988; McNider *et al*., 1988; Moran and Pielke, 1996; Gupta *et al.*, 1997) have found that the time and space resolution of meteorological data fields are important to mesoscale (20 to 2000 km) dispersion modeling. Brost *et al.* (1988) found that increasing the spatial density and temporal resolution (from 12 to 6 hr) of meteorological data improved mesoscale dispersion simulations of the CAPTEX experiment. McNider *et al.* (1988) and Moran and Pielke (1996) showed that resolving the diurnal (24 hr) and inertial periods (e.g., 15.6 hr at 50 deg) in mesoscale dispersion simulations can be important. McNider *et al.* showed that this may be due to variations in vertical turbulent mixing in the boundary layer along with vertical shear in the horizontal wind that occur during these periods.

This paper presents the results from a series of numerical experiments designed to investigate the effect of temporal and spatial resolution of meteorological data on operational dispersion model simulations. In these numerical experiments, simulations with the RDM-ADPIC dispersion model were made with different meteorological data fields: NOGAPS data (as used in the real-time study), ECMWF data (as used in ATMES II), and ECMWF data with decreased space, time and vertical resolution. The results of simulations are compared to ground-level air concentrations measured during ETEX. Section 2 describes the models and input data used to perform the simulations. Section 3 presents the results of the numerical experiments. Section 4 summarizes and discusses the results.

2. MODELS

2.1 Meteorological models

Meteorological data fields from two numerical weather prediction models were used in this work. The NOGAPS model (Hogan and Rosmond, 1991) is a T159 spectral model with 18 vertical levels through the entire atmosphere. The NOGAPS data used in this work are analysis and forecasts of the mean wind supplied at 2.5 degree latitude, longitude horizontal resolution (average resolution of approximately 225 km), at the standard vertical pressure levels, and at 12-hr intervals (analysis at 1200 UTC on 23 Oct. 1994 and subsequent 12-hourly forecasts to 0000 UTC on 26 Oct.) obtained from the U.S. Navy Fleet Numerical and Meteorology and Oceanography Center (FNMOC). The ECMWF model is a T213 spectral model with 31 vertical levels between the surface and 30 km (ECMWF, 1995). The ECMWF data used in this work are analyses of mean wind, temperature, and pressure supplied at 0.5 degree horizontal resolution (average resolution of approximately 45 km), at 14 vertical levels below 500 mb, and at 6 hr intervals (1800 UTC, 23 Oct. to 0600 UTC, 27 Oct. 1994).

2.2 Dispersion model

The basic framework of the dispersion model used in this work is the same as that of the ADPIC model described by Lange (1989). Both the ADPIC model and the newer RDM-ADPIC model utilize the conservation of species principle expressed in the form of the 3-D advection-diffusion equation:

$$\frac{\partial \overline{C}}{\partial t} = -\overline{u}\,\frac{\partial \overline{C}}{\partial x} - \overline{v}\,\frac{\partial \overline{C}}{\partial y} - \overline{w}\,\frac{\partial \overline{C}}{\partial z} + \frac{\partial}{\partial x}\left(K_x \frac{\partial \overline{C}}{\partial x}\right) + \frac{\partial}{\partial y}\left(K_y \frac{\partial \overline{C}}{\partial y}\right) + \frac{\partial}{\partial z}\left(K_z \frac{\partial \overline{C}}{\partial z}\right) \tag{1}$$

where $\overline{C}$ is the mean air concentration of the species; $\overline{u}$, $\overline{v}$, and $\overline{w}$ are the mean wind components in the *x*, *y*, and *z* directions, respectively; *t* is time; and K_x, K_y, and K_z are the eddy diffusivities for the three coordinate directions.

The RDM-ADPIC model solves the advection-diffusion equation using a Lagrangian stochastic, random displacement method, and was used in this work. This method was implemented and validated versus analytic solutions by Ermak *et al.* (1995). It uses the following stochastic differential equations for the change in fluid particle position in the three coordinate directions:

$$dx = \overline{u}\,dt + (2K_x)^{1/2}\,dW_x\,, \tag{2a}$$

$$dy = \overline{v}\,dt + (2K_y)^{1/2}\,dW_y, \tag{2b}$$

$$dz = \overline{w}\,dt + \frac{\partial K_z}{\partial z}\,dt + (2K_z)^{1/2}\,dW_z, \tag{2c}$$

where $dW_{x,y,z}$ are three independent random variates with zero mean and variance *dt*, i.e.,

$$\overline{dW} = 0,$$
$$\overline{dW^2} = dt.$$

Eqs. (2a-b) assume that the spatial derivatives of the eddy diffusivities in the horizontal directions can be neglected. Eqs. (2a-c) are integrated in time to calculate particle trajectories in Monte Carlo simulations. Mean air concentrations are calculated from the distribution of particle positions and the source distribution term. Some of the benefits of the Lagrangian random displacement method approach, compared to the hybrid Eulerian-Lagrangian particle-in-cell method in ADPIC, are that a sub-grid diffusion approximation is no longer needed, and numerical accuracy of the diffusion calculation is improved because particle displacement does not depend on the resolution of the Eulerian grid used to calculate species concentration.

The mean horizontal wind components were obtained from the NOGAPS and ECMWF data by interpolating them to the RDM-ADPIC meteorological data grid using an inverse-distance-squared weighting method in the horizontal, and linear interpolation in the vertical direction. The vertical mean wind component was not used. The RDM-ADPIC grid domain covered 2500×2500 km in the horizontal directions and 2100 m in the vertical direction. A uniformly spaced grid with 51×51 node points in the horizontal and 31 node points in the vertical direction (50 $\times$ 50 km resolution in the horizontal and 70 m resolution in the vertical) was used in all simulations.

The vertical eddy diffusivity parameterization described by Lange (1989) was used, in which $K_z(z)$ is calculated from boundary-layer and surface-layer similarity theory relationships using turbulence scaling parameters (friction velocity, Obukhov length and boundary layer depth). Above the boundary layer, a constant value of K_z = 0.01 m^2 s^{-1} was used. The horizontal eddy diffusivities were based on the long-range, semi-empirical relationship for the travel-time-dependent horizontal standard deviation of the concentration distribution, $\sigma_y(t)$, determined by Rodriguez *et al*. (1995), along with the relationships $K_y = \frac{1}{2}\left(d\sigma_y^2/dt\right)$, and $K_x = K_y$.

The boundary layer depths for input to the dispersion model were determined from an analysis of the vertical profiles of the ECMWF wind and temperature data from several locations in the experiment region. The depth of the ground-based nocturnal temperature inversion was used as one criterion for the depth of the nighttime boundary layer. The height of the elevated temperature inversion was used as a criterion for the depth of the daytime boundary layer. In addition, the height at which the winds approached a fairly uniform profile (the geostrophic level) was used as a criterion for the boundary layer depth during both daytime and nighttime periods. Based on this analysis, a representative daytime boundary layer depth of 1000 m was used for all daytime periods, from 0800 to 1600 UTC. Nighttime boundary layer depths ranging from 500 to 400 m were used from 1600 to 0800 UTC. An Obukhov length value of –100 m (slightly unstable) was used during daytime, and 100 m (slightly stable) was used during nighttime.

For the first ETEX experiment, used in this work, the perfluorocarbon tracer gas was released with an emission rate of 7.95 g s^{-1} near ground level for an 11 hr 50 min period starting at 23 Oct. 1994, 1600 UTC. In each simulation, 30000 marker particle trajectories were calculated. Particle positions were sampled and used to calculate air concentrations on the same grid as used for the mean wind, except that four additional nested grids were used in the near-source region. These four nested grids had 3.125, 6.25, 12.5, and 25 km horizontal resolution, and extended to approximately 60, 125, 250 and 500 km, respectively, downwind of the source.

3. NUMERICAL EXPERIMENTS

To study the importance of the spatial and temporal resolution of the mean wind on the accuracy of dispersion simulations, a series of six simulations were completed and compared. These six experiments (designated Test 1 through 6) differed only in the meteorological model used and the spatial and temporal resolution of the meteorological data, and can be summarized as follows:

- *Test 1*: NOGAPS data at 2.5 degree horizontal resolution, 12 hr intervals, and four standard pressure levels: 1000, 925, 850 and 700 mb.

- *Test 2*: ECMWF data at 0.5 degree horizontal resolution, 6 hr intervals, and seven vertical levels: approximately 30, 150, 350, 640, 950, 1380, 1750, and 2200 m above ground level.

- *Test 3*: ECMWF data with lower *vertical* resolution, using only four vertical levels, corresponding to the levels closest to the four standard pressure levels (second, fourth, sixth and tenth ECMWF levels.)

- *Test 4*: ECMWF data with lower *temporal* resolution, using only data at 12 hr intervals (0000 and 1200 UTC.)

- *Test 5*: ECMWF data with lower *horizontal* resolution, using data from every fifth node point to simulate 2.5 degree horizontal resolution.

- *Test 6*: ECMWF data with a combination of lower vertical resolution (as in Test 3), temporal resolution (as in Test 4) and horizontal resolution (as in Test 5.)

Test 1 used the same mean wind data as used in the real-time model evaluation phase of ETEX. The Test 2 simulation used the same mean wind data as in the ATMES II model evaluation study. Tests 3, 4, 5, and 6 were designed to assess the relative importance of vertical, temporal and horizontal resolution for dispersion simulations.

The air concentrations at the near-ground sampling sites during the first 60 hours of the experiment period were compared to model calculations from each of the 6 simulations in two ways. First, contour maps of measured and calculated concentrations were compared visually. Second, the percentage of calculated concentrations within factors of 2, 5, and 10 of measured near-surface concentrations (paired in space and time) were calculated. (To be within a factor of n the ratio of measured concentration to calculated concentration, R, must be in the range $\frac{1}{n} < R < n$.) Only data for measurement locations and times with non-zero measured concentrations (after background concentration was subtracted) were used in this second analysis. This resulted in 664 data points being used.

Figures 1a, b and c show contours of the 3-hr average tracer air concentration measured at sampling sites during the first ETEX experiment for periods ending 24, 36 and 48 hr, respectively, after the beginning of the simulation. It is important to note that the contours in Fig. 1 were produced using measured data from the sampling sites, while the contours in the other figures (Figs. 2, 3 and 4) were produced using model-calculated data on the model grid. Therefore, the contours shown in Fig. 1 may not be representative of the concentration pattern in regions poorly sampled by the sampling site network (this is at least partially responsible for the gap in the contours over France in Fig. 1a.)

Figures 2a, b and c show contours predicted by the RDM-ADPIC simulation using the NOGAPS data (Test 1) at 24, 36, and 48 hr. Figures 3a, b and c show the results of RDM-ADPIC simulation using the ECMWF data (Test 2). It can be seen from these figures that the simulations using the ECMWF data are in better agreement with the measured concentrations. In particular, the Test 2 simulation produced much better predictions of the tracer concentration field at 24 and 36 hr over northern France, Belgium, The Netherlands, and Germany and at 48 hr over northern Germany and southern Scandinavia. At 24 and 36 hr, the simulations using the NOGAPS data failed to simulate observed transport of the material into Belgium and The Netherlands, and erroneously predicted a lobe of the concentration field extending into Switzerland and Austria. The improved results with the ECMWF data are also reflected in the statistics given in Table 1, which show that the simulation using the ECMWF data resulted in a significantly higher percentage of calculated concentration values within a factor of 2, 5 and 10 of measured values.

Table 1 also gives the statistical results of simulations with ECMWF data with decreased temporal, vertical, and horizontal resolution. Decreasing the number of vertical levels from 7 to 4 (Test 3) resulted in a small decrease in the percentage of calculated values within a factor of 2, 5 and 10 of measured values. However, the two simulations using an increased data interval of 12 hr (Test 4) and a decreased horizontal resolution of 2.5 deg (Test 5) resulted in a more significant drop in these percentages (a change greater than approximately 5% is statistically significant.) The simulation with a combined decrease in the horizontal, vertical and temporal resolution of the ECMWF data (Test 6) shows a marked decrease in the percentages within a factor of 2, 5, and 10 compared to all the other simulations using ECMWF data.

Figures 4a, b and c show contours of the 3-hr average tracer air concentration predicted by the Test 6 simulation for periods ending at 24, 36 and 48 hr. These predicted concentrations show poorer agreement with the measured concentrations (Fig. 1a-c) than the simulations using all the ECMWF data (Test 2, Figs. 3a-c), but are still in significantly better agreement with the measured concentrations than the results of the simulations using the NOGAPS data (Test 1, Figs. 2a-c).

It is not surprising that the lower resolution simulation using ECMWF data (Test 6) are better than the lower resolution simulations using NOGAPS data (Test 1). Even after data is removed from the ECMWF fields (as in Tests 3, 4, 5, and 6), the remaining data points were still based on a higher-resolution prognostic simulation than the NOGAPS data. In addition, all the ECMWF data periods were from analyses, whereas the NOGAPS data were from an analysis and forecasts. Although, in the previous, real-time study, simulations with analysis-only NOGAPS data did not significantly change the agreement with measurements compared to simulations using NOGAPS analysis and forecasts.

4. SUMMARY AND DISCUSSION

The use of analyzed mean wind fields from the higher resolution ECMWF model produced significantly better agreement between the Lagrangian particle dispersion model predicted concentrations and the ETEX measurements than the use of forecast, lower resolution NOGAPS mean wind data. In numerical experiments using the ECMWF data, degrading the horizontal resolution alone, from 0.5 deg (approx. 45 km) to 2.5 deg (approx. 225 km), or the temporal resolution alone, from 6 to 12 hr intervals, resulted in greater decreases in the accuracy of dispersion simulations than degrading the vertical resolution from 7 to 4 levels. Degrading the horizontal, vertical and temporal resolution of the ECMWF data together resulted in an even greater decrease in the accuracy of the dispersion simulations.

The improved results with 0.5 instead of 2.5 degree horizontal resolution indicate that circulations with horizontal scales resolved at 45 km, but not at 225 km, made an important contribution to mesoscale dispersion. Similarly, temporal variations resolved at 6 hr, but not at 12 hr intervals, were important. These results indicate that the resolution of the diurnal cycle with at least 6 hr interval data may be important to mesoscale dispersion simulations, as found in previous studies cited in section 1. Improved horizontal and temporal resolution may have been critical during the beginning of the experiment when a short wave disturbance, with wavelength of approximately 300 km in the surface pressure field, passed the release site during the 12 hr release period (Esser and Builtjes, 1997) and moved eastward through northern France. This disturbance was at least partially resolved at the 45 km grid spacing and 6 hr intervals of the ECMWF data, but not at the 225 km grid spacing and 12 hr intervals of the NOGAPS data. Flow with a stronger northward component was present to the east of the low pressure trough associated with this disturbance. As a consequence, simulations with ECMWF data were better able to simulate the northward transport into Belgium and The Netherlands during the first 36 hours of the experiment.

This work shows that increasing the resolution of meteorological fields provided to a Lagrangian particle dispersion model has the potential to improve predictions of hazardous material air concentrations for emergency response applications. With increased computer power and data transfer rates, the use of higher resolution meteorological models has become practical for emergency response calculations. Since the real-time phase of ETEX, the ARAC program has begun to use higher resolution global prognostic model data (e.g., 1 degree, 6 hourly NOGAPS data obtained from the FNMOC), and still higher resolution mesoscale prognostic model data (Albritton *et al.*, 1997) in its operational emergency response system.

This study has been limited to the first ETEX experiment. With the exception of the short wave disturbance noted and some moist convection, the flow was dominated by synoptic-scale forcing. During more complex meteorological conditions that are significantly influenced by the presence of smaller mesoscale circulations (e.g., frontal circulations, land and sea breeze circulations), accurate, higher-resolution meteorological fields are likely to be even more important to dispersion simulations.

Acknowledgments — This research was performed under the auspices of the U.S. Department of Energy at Lawrence Livermore National Laboratory under contract number W-7405-Eng-48. The authors thank H. Walker for his work in processing data used in this study, and K.T. Foster and Dr. G.A. Sugiyama for valuable discussions on statistical analysis. We also thank the European Commission (JRC-Ispra), IAEA, and WMO for providing the ETEX data set, and the EC JRC-Ispra and Enviroware srl for providing Figs. 1a-c.

REFERENCES

Albritton, J.R., R.L. Lee, R. Hodur, C.-S. Liu (1997) Modeling the wind fields of accidental releases by mesoscale modeling. *Proceedings, Sixth Topical Meeting on Emergency Response*, San Francisco, CA, April 1997, pp. 359-363. American Nuclear Society, Inc., La Grange Park, IL.

Brost, R.A., P.L. Haagenson, and Y.-H. Kuo (1988) Eulerian simulation of tracer distribution during CAPTEX. *J. Appl. Meteorol.*, **27**, 579-593.

ECMWF (1995) *The ECMWF/ETEX Data Set*. European Center for Medium-Range Weather Forecasts, Shinfield Park, Reading RG2 9AX, UK.

Ermak, D.L., J.S. Nasstrom, and A.G. Taylor (1995) *Implementation of a Random Displacement Method (RDM) in the ADPIC Model Framework*. Report UCRL-ID-121742, Lawrence Livermore National Laboratory, Livermore, CA, 16 pp.

Esser, P.J. and P.J.H. Builtjes (1997) The local meteorological situation during the ETEX experiments. *ETEX Symposium on Long-range Atmospheric Transport, Model*

Verification and Emergency Response, Proceedings, 13-16 May 1997, Vienna, Austria (K. Nodop, ed.). EUR 7346 EN, Office for Official Publications of the European Communities, Luxembourg. pp. 63-66.

Gudiksen, P.H., T.F. Harvey, and R. Lange (1989) Chernobyl source term, atmospheric dispersion and dose estimation. *Health Physics*, **57**, pp. 697-706.

Gupta, S., R.T. McNider, M. Trainer, R.J. Zamora, K. Knupp, and M.P. Singh (1997) Nocturnal wind structure and plume growth rates due to inertial oscillations. *J. Appl. Meteorol.*, **36**, 1050-1063.

Girardi, F., G. Graziani, W. Klug, and K. Nodop (1997) The European tracer experiment description and summary of the ETEX project. *ETEX Symposium on Long-range Atmospheric Transport, Model Verification and Emergency Response, Proceedings*, 13-16 May 1997, Vienna, Austria (K. Nodop, ed.). EUR 7346 EN, Office for Official Publications of the European Communities, Luxembourg. pp. 83-86.

Hogan, T.F. and T.E. Rosmond (1991) The description of the navy operational global atmospheric prediction system's spectral forecast model. *Mon. Wea. Rev.*, **119**, 1789-1815.

Lange, R. (1989) Transferability of a Three-Dimensional Air Quality Model between Two Different Sites in Complex Terrain. *J. Appl. Meteorol.*, **28**, 7, 665-679

McNider, R.T., M.D. Moran, and R.A. Pielke (1988) Influence of diurnal and inertial boundary-layer oscillations on long-range dispersion. *Atm. Environ.*, **22**, 2445-2462.

Moran, M.D., and R.A. Pielke (1996) Evaluation of a mesoscale atmospheric dispersion modeling system with observations from the 1980 Great Plains mesoscale tracer field experiment. Part II: Dispersion simulations. *J. Appl. Meteorol.*, **35**, 308-329.

Nasstrom, J.S., 1995: *Turbulence Parameterizations for the Random Displacement Method Version of ADPIC*. Report UCRL-ID-120965, Lawrence Livermore National Laboratory, Livermore, CA. 22 pp.

Nodop, K., R. Connolly, and F. Girardi (1997) The European tracer experiment – experimental results and database. *ETEX Symposium on Long-range Atmospheric Transport, Model Verification and Emergency Response, Proceedings*, 13-16 May 1997, Vienna, Austria (K. Nodop, ed.). EUR 7346 EN, Office for Official Publications of the European Communities, Luxembourg. pp. 59-62.

Rodriguez, D.J., H. Walker, N. Klepikova, A. Kostrikov, and Y. Zhuk (1995) Evaluation of two pollutant dispersion models over continental scales. *Atmos. Environ.*, **29**, 799-812.

Sullivan, T.J., J.S. Ellis, C.S. Foster, K.T. Foster, R.L. Baskett, J.S. Nasstrom, and W.W. Schalk III (1993) Atmospheric Release Advisory Capability: Real-time modeling of Airborne Hazardous Material. *Bulletin of the Amer. Meteorol. Soc*., **74**, 2343-2361.

Table 1. Summary of meteorological data used in the RDM-ADPIC dispersion model simulations and the resulting percentage of predicted concentrations within factors of 2, 5, and 10 of the measured concentrations, for each of the six tests described in Section 3.

		Meteorological data			Dispersion model predictions		
Test	Model	Horizontal resolution (deg)	Data interval (hr)	Number of vertical levels	Factor of 2 (%)	Factor of 5 (%)	Factor of 10 (%)
1	NOGAPS	2.5	12	4	15.5	37.2	47.1
2	ECMWF	0.5	6	7	29.3	55.2	65.7
3	ECMWF	0.5	6	4	28.2	52.5	62.9
4	ECMWF	0.5	12	7	24.5	49.2	61.0
5	ECMWF	2.5	6	7	24.1	51.8	61.6
6	ECMWF	2.5	12	4	22.7	45.1	55.7

Figure captions (figure numbers are on back of each page)

Figure 1. Contours of 3-hr average air concentration measured at sampling sites for periods ending (a) 24 hr, (b) 36 hr, and (c) 48 hr after the beginning of simulation (respectively, 24 Oct., 1200-1500 UTC; 25 Oct., 0000-0300 UTC; and 25 Oct., 1200-1500 UTC). Contour levels are 0.01 (outermost), 0.1, and 0.5 (innermost) ng m^{-3}.

Figure 2. Contours of 3-hr average air concentration predicted by RDM-ADPIC using NOGAPS mean wind data (Test 1 simulation). Time periods are the same as in Fig. 1: (a) 24 hr, (b) 36 hr, and (c) 48 hr after the beginning of the simulation. Contour levels are 0.01 (outermost), 0.1, and 0.5 (innermost) ng m^{-3}, as in Fig. 1.

Figure 3. Same as Fig. 2, expect using ECMWF mean wind data (Test 2 simulation).

Figure 4. Same as Fig. 2, expect using ECMWF mean wind data with lower vertical resolution, temporal resolution and horizontal resolution (Test 6 simulation).

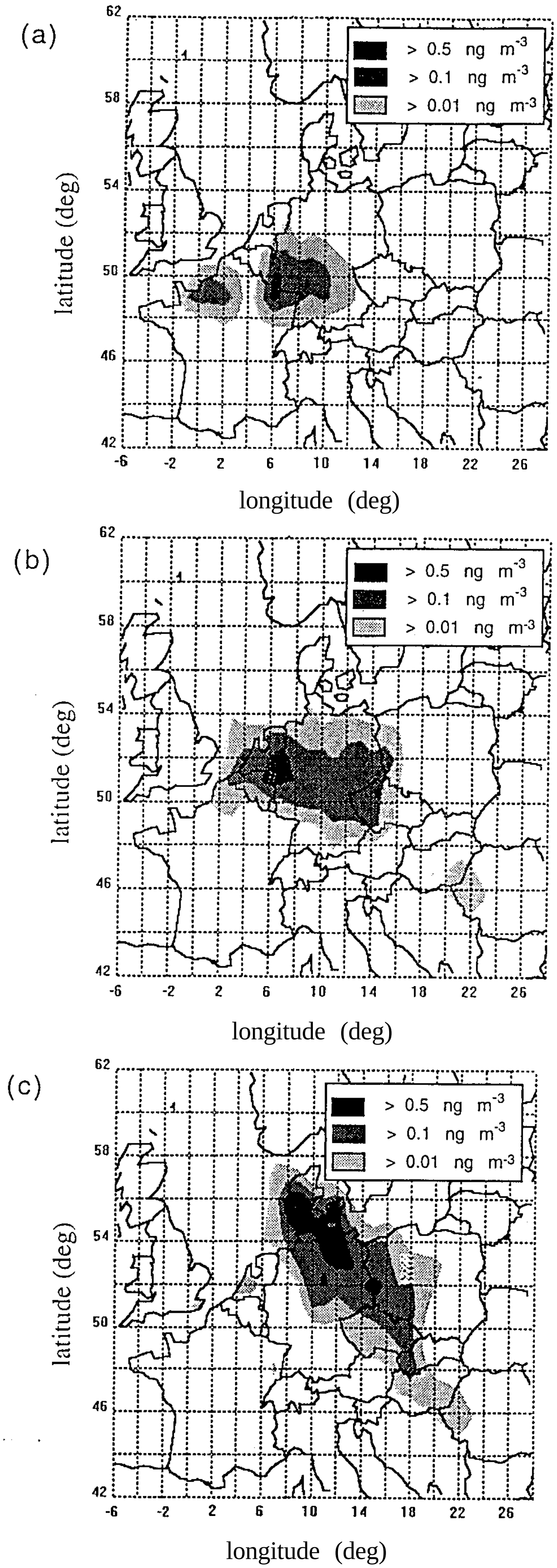

Figure 1. Contours of 3-hr average air concentration measured at sampling sites for periods ending (a) 24 hr, (b) 36 hr, and (c) 48 hr after the beginning of simulation (respectively, 24 Oct., 1200-1500 UTC; 25 Oct., 0000-0300 UTC; and 25 Oct., 1200-1500 UTC). Contour levels are 0.01, 0.1, and 0.5 ng m-3.

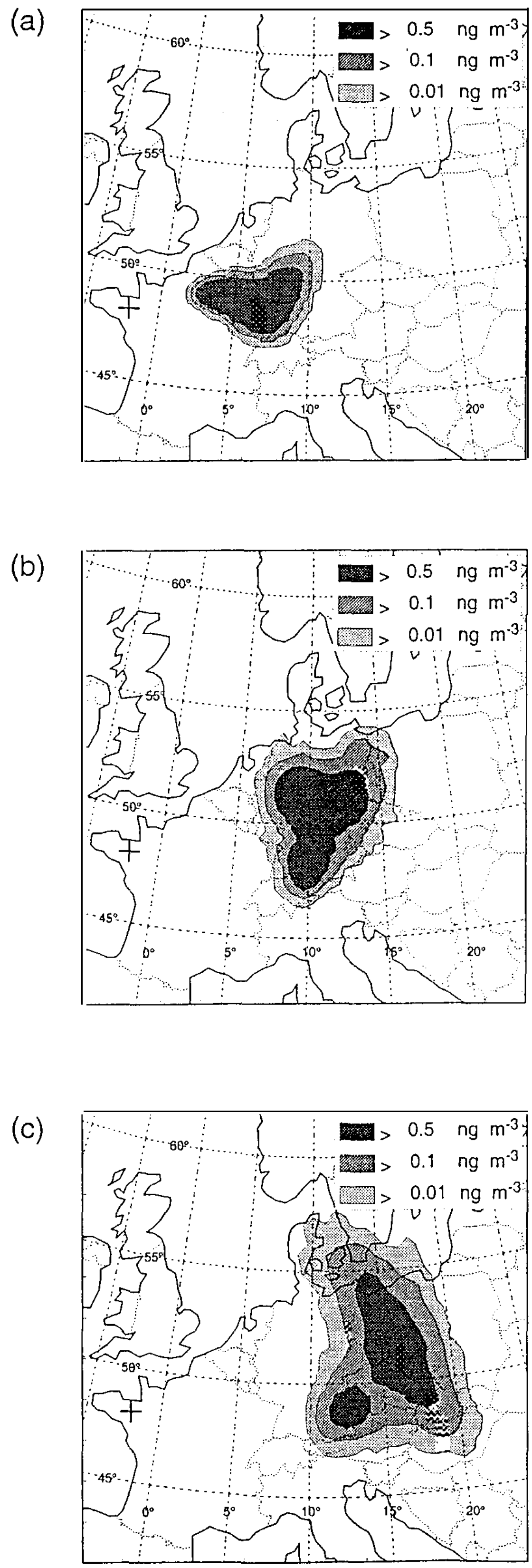

Figure 2. Contours of 3-hr average air concentration predicted by RDM-ADPIC using NOGAPS mean wind data (Test 1 simulation). Time periods are the same as in Fig. 1: (a) 24 hr, (b) 36 hr, and (c) 48 hr after the beginning of the simulation. The "+" symbol in northwestern France shows the source location. Contour levels are 0.01, 0.1, and 0.5 ng m^{-3}, as in Fig. 1.

(a)

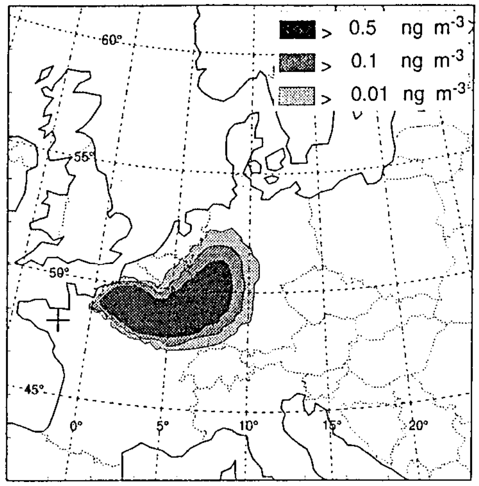

(b)

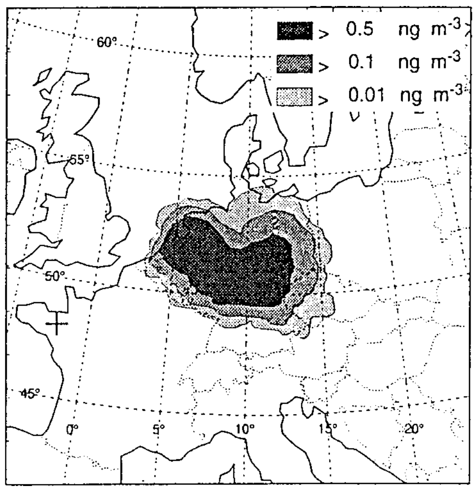

(c)

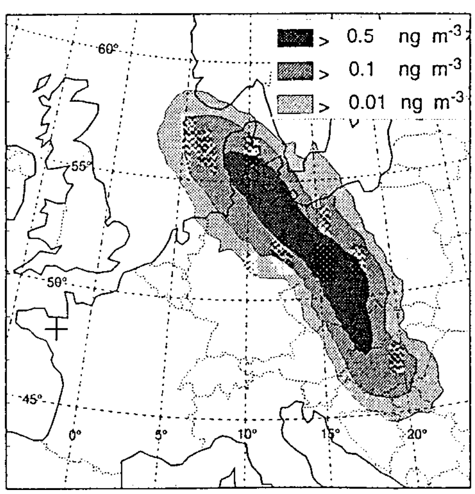

Figure 3. Same as Fig. 2, expect using ECMWF mean wind data (Test 2 simulation).

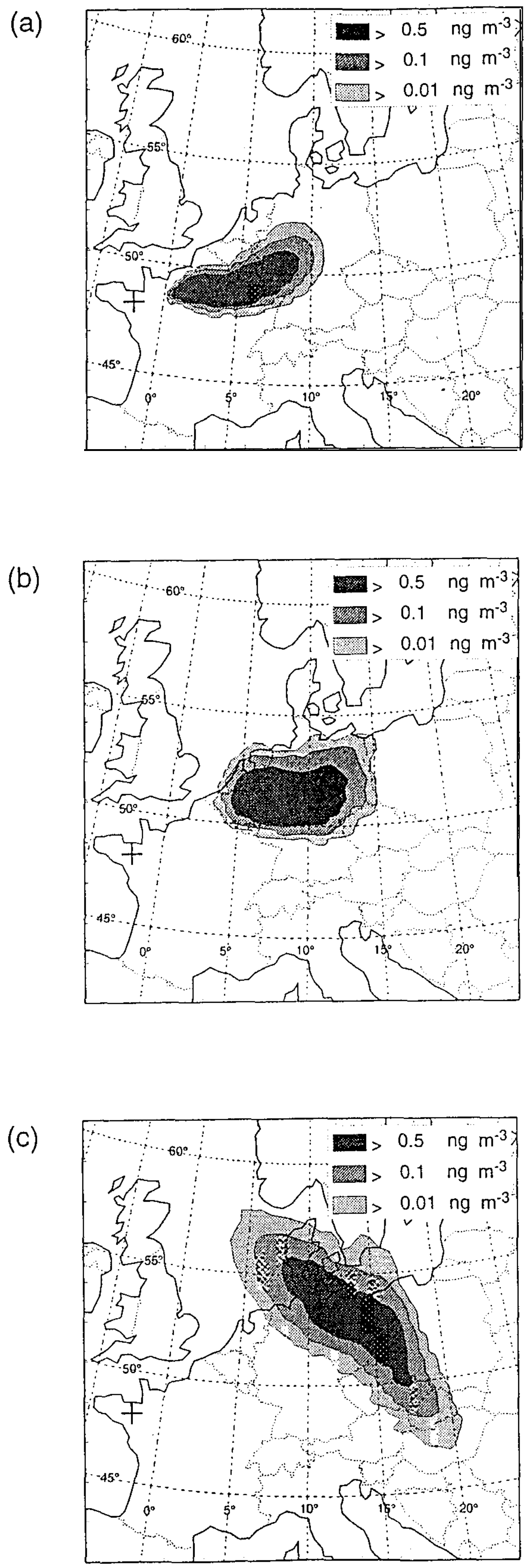

Figure 4. Same as Fig. 2, expect using ECMWF mean wind data with lower vertical resolution, temporal resolution and horizontal resolution (Test 6 simulation).